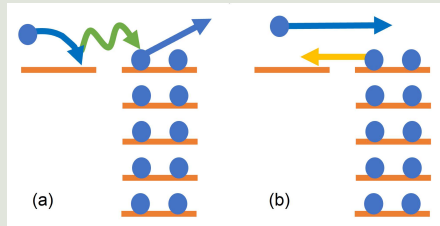


V. Graves¹, J. Šenk^{2,3}, P. Kolorenč³, N. Sisourat² and J. D. Gorfinkel¹
¹The Open University, Walton Hall, Kents Hill, Milton Keynes, MK7 6AA, UK, ²Sorbonne Université, CNRS, Laboratoire de Chimie Physique-Matière et Rayonnement, F-75005 Paris, France, ³Institute of Theoretical Physics, Faculty of Mathematics and Physics, Charles University Prague, Czech Republic

1. Introduction

Interparticle Coulombic Electron Capture (ICEC) is an environment enabled process that involves an electron being captured by an atom, a molecule or a quantum dot [1]. When the electron is captured, the excess energy is released leading to the ionization or excitation of a nearby particle. Here, we focus on ionization:



Two mechanisms contribute to the overall ICEC process: (a) **virtual photon exchange**: an electron is captured from the continuum and a virtual photon is exchanged; (b) **electron transfer**: the environment (a neighbouring atom or molecule) provides the electron (i.e. no capture of the projectile electron takes place).

ICEC was first predicted in 2009 [2] and can lead to cross sections that are significantly larger than those for conventional photorecombination.

2. Systems investigated

We studied [3] ICEC for:

ICEC-P:



ICEC-W:



3. Target states

The ICEC cross sections (see right) are strongly dependent on the distance between electron acceptor and neighbour. We modelled states of $H^+ + H_2O$ and $H + H_2O^+$ up 18 eV for a range of distances R .

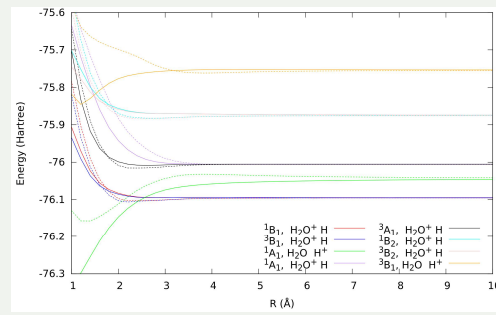


Figure 1: Target state energies as a function of R for lowest 8 target states. Solid lines, H2OH orientation; dashed, HH2O.

Symmetry	State	$R = 3 \text{ \AA}$	$R = 8 \text{ \AA}$	$R = 25 \text{ \AA}$	$R = \infty$
1	3B_1	$H(1s) H_2O^{+1} (X^2B_1)$	0.0000	0.0000	0.0000
2	1B_1	$H(1s) H_2O^{+1} (X^2B_1)$	0.0035	0.0108	0.0000
3	1A_1	$H^+ H_2O^{+1} (A_1)$	0.5513	1.5665	1.2960
4	3A_1	$H(1s) H_2O^{+1} (A_1)$	2.3717	2.4161	2.4390
5	1A_1	$H(1s) H_2O^{+1} (A_1)$	2.5102	3.0279	2.4500
6	3B_2	$H(1s) H_2O^{+1} (B_2)$	6.0979	5.9543	6.0190
7	1B_2	$H(1s) H_2O^{+1} (B_2)$	6.1017	5.9564	6.0190
8	3B_1	$H^+ H_2O^{+1} (B_1)$	9.2026	9.5559	9.3040
9	1B_1	$H^+ H_2O^{+1} (B_1)$	9.8144	10.170	9.9090
10	3A_1	$H^+ H_2O^{+1} (A_1)$	11.992	12.135	11.847
11	1A_1	$H^+ H_2O^{+1} (A_1)$	13.005	13.248	12.903
12	3B_2	$H^+ H_2O^{+1} (B_2)$	14.192	14.302	14.198
13	1B_2	$H^+ H_2O^{+1} (B_2)$	15.191	15.018	14.950
14	3B_1	$H^+ H_2O^{+1} (B_1)$	15.017	15.341	14.982
15	1B_2	$H^+ H_2O^{+1} (B_2)$	15.683	16.380	15.882
16	3B_1	$H(1s) H_2O^{+1} (B_1)$	15.770	15.505	15.982
17	3A_1	$H^+ H_2O^{+1} (A_1)$	16.526	17.011	16.642
18	1A_1	$H^+ H_2O^{+1} (A_1)$	16.490	16.127	16.642
19	3B_1	$H^+ H_2O^{+1} (B_1)$	16.967	17.227	17.198
20	1B_1	$H(1s) H_2O^{+1} (B_1)$	17.015	17.440	17.198

4. R-Matrix Method and model

The R-Matrix method solves the time independent Schrödinger equation by splitting the problem into two regions, separated by a sphere of radius a . Here, the UKRMol+ [4] suite of codes is used. The inner region multi-electronic scattering ($N + 1$) wavefunction can be expanded using the Close-Coupling approximation:

$$\Psi^{N+1} = \mathcal{A} \sum_{i,j} a_{i,j} \phi_i^N \eta_{i,j} + \sum_j b_j \phi_j^{N+1}$$

$a_{i,j}, b_j$ = Expansion coefficients obtained from the diagonalization of the $N+1$ Hamiltonian.

ϕ_i^N = N -electron target electronic wavefunction.

$\eta_{i,j}$ = Continuum orbital.

ϕ_j^{N+1} = L^2 functions built from occupied and virtual orbitals (VOs). Used to describe polarization effects.

A complete active space consisting of 9 active orbitals and 8 active electrons and HF orbitals generated with the cc-pVQZ basis set were used for the target. The close-coupling included 20 target states. The continuum contained BTOs only with the parameters presented below.

$a=20 \text{ \AA}$ a_0 No. BTOs: 20 No. partial waves: 6 BTO order: 6 1/2-el Legendre expansion: 85/30

6. R-dependence

The asymptotic formula [2] models the virtual photon exchange when there is no interaction between acceptor and neighbour:

$$\sigma_{ICEC}(E) = \frac{3 \hbar^4 c^4}{4\pi} \frac{\sigma_{PI}^B(E')}{R^6(h\nu)^4} \sigma_{PR}^{A^+}(E) = \frac{3 \hbar^4 c^2}{8\pi m_e g_{A^+}} \frac{g_A \sigma_{PI}^A(E) \sigma_{PI}^B(E')}{ER^6(h\nu)^2}$$

• Electron transfer depends on orbital overlap [5] so is proportional to $\exp(-R^2)/R^2$

• R-dependence is stronger for electron transfer

• Orientation dependence is stronger for electron transfer

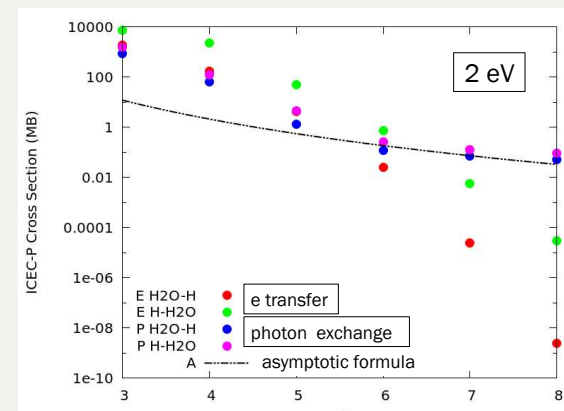


Figure 4: R dependence of the electron transfer and virtual photon exchange cross sections for 2 eV and both orientations.

References & Acknowledgments

[1] Bande, Fasshauer, Molle, Peláez, Pont and Sisourat (2023), J. Phys. B: At. Mol. Opt. Phys. **56** 232001

[2] Gokhberg and Cederbaum, J. Phys. B: At. Mol. Opt. Phys. **42** 231001 (2009); PRA. **82**, 052707 (2010)

[3] Graves, Šenk, Kolorenč, Sisourat, Gorfinkel (2024), J. Chem. Phys. **160**, 204306

[4] Mařín, Benda, Gorfinkel, Harvey and Tennyson (2020), Comput. Phys. Commun. **249**, 107092

[5] Šenk, Graves, Gorfinkel, Kolorenč, Sisourat, (2024), J. Chem. Phys. **161**, 174113

[6] Molle, Dubois, Gorfinkel, Cederbaum and Sisourat, (2021), Phys. Rev. A **103** 012808

5. Mechanisms

- Approximate separation (neglecting interference) of the mechanisms in R-matrix calculations enables the evaluation of a virtual photon exchange and an electron transfer cross section.
- As $R \downarrow$, electron transfer increases faster than virtual photon exchange
- Electron transfer dominates for $R < 6$
- Electron transfer more effective if H⁺ is on the H end of H₂O (HH₂O)
- Geometry effect larger for larger R: strong effect on electron transfer when $R \uparrow$, much smaller on photon exchange for all R
- In ICEC-W ratios are all > 1

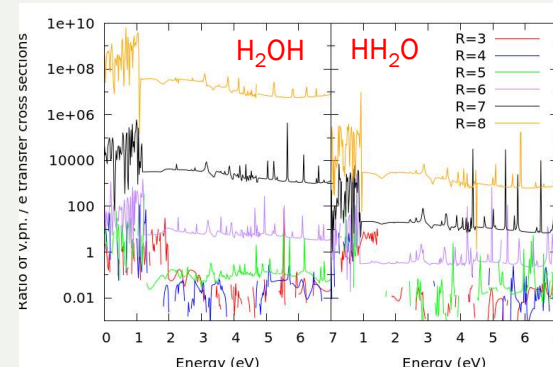


Figure 2: Ratio of the virtual photon exchange and electron transfer cross sections for ICEC-P for both relative orientations for the acceptor-neighbour distances, R , in Å, indicated in the panels.

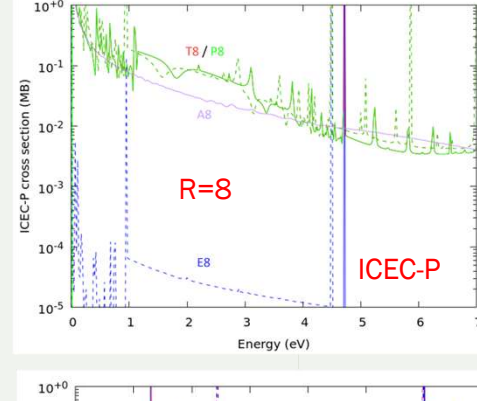
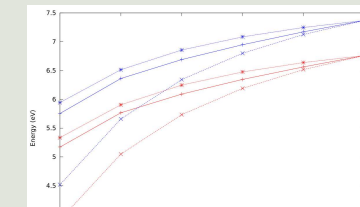


Figure 3: Cross sections for virtual photon exchange (P), electron transfer (E) and 'total' ICEC (T) for $R=8 \text{ \AA}$ (left) and $R=3 \text{ \AA}$ (right) for both orientations: H2OH (solid line), HH2O (dashed line)

7. Resonances

Many resonances are seen in the ICEC cross section, mainly associated to Rydberg states of H₂O. We identified [6] two 2A_1 and two 2A_2 resonances with a strong dependence on R at approximately the same energy for ICEC-P and ICEC-W and both orientations.

R-dependence indicates partial ion-pair character



Dyson orbitals indicate partial H + H₂O* (³B₁) and H⁺ + H₂O^{-(1A₁)} character at small R whereas at large R, H^{q+} + H₂O^{-(1A₁)} dominates completely



Figure 5: 2A_1 contribution to the ICEC cross sections for ICEC-P (top) and ICEC-W (bottom) for a range of R and both orientation (full and dashed lines). Red circles highlight the lower resonance and blue circles highlight the higher resonance



8. Conclusions

- Both virtual photon exchange and electron transfer are sensitive to the energetics of the system.
- The electron transfer mechanism is significant for a range of acceptor-neighbour distances and makes the largest contribution to the ICEC cross section at smaller R
- The magnitude of the electron transfer cross section depends strongly on the relative position of acceptor and neighbour. The photon transfer cross section t is fairly insensitive to it.
- Although the orientation dependence of the electron transfer is stronger for larger R, its smaller contribution to ICEC means the ICEC cross section is more orientation dependent for small R.
- The difference between the asymptotic cross section and the *ab initio* cross section is due almost completely to the electron transfer process.
- The electron transfer mechanism doesn't change the spin of the target whereas virtual photon exchange does. This points at a potential way of establishing experimentally whether virtual photon exchange takes place.
- A rich resonance spectrum is visible in the ICEC cross section, including resonances with ion-pair character that deserve further investigation.

V. G. acknowledges support from the EPSRC Doctoral Training Partnership EP/T518165/1. N.S. and J.S. thank the ANR-DFG for financial support of the QD4ICEC project: the ANR grant is ANR-22-CE92-0071-01